

# <sup>1</sup> Quantifying the sources of spread in climate change <sup>2</sup> experiments

O. Geoffroy,<sup>1</sup> D. Saint-Martin<sup>1</sup> and A. Ribes<sup>1</sup>

---

<sup>1</sup>Centre National de Recherches  
Météorologiques (CNRM-GAME),  
Toulouse, France

3 Energy-balance models (EBM) constitute a useful framework for summa-  
4 rizing the first-order physical properties driving the magnitude of the global  
5 mean surface air temperature response to an externally imposed radiative  
6 perturbation. Here the contributions of these properties to the spread of the  
7 temperature responses of an ensemble of coupled Atmosphere-Ocean Gen-  
8 eral Circulation Models (AOGCM) of the fifth phase of the Coupled Model  
9 Intercomparison Project (CMIP5) are evaluated within the framework of a  
10 state-of-the-art EBM. These partial contributions are quantified (in equilib-  
11 rium and transient conditions) using the analysis of variance method. The  
12 radiative properties, particularly the strength of the radiative feedback to  
13 the global equilibrium surface warming, appear to constitute the most pri-  
14 mary source of the spread.

## 1. Introduction

15 The equilibrium climate sensitivity ECS (the equilibrium mean surface air tempera-  
16 ture response to a doubling of carbon dioxide concentration) and the transient climate  
17 response TCR (the temperature response at the time of  $2\times\text{CO}_2$  in a  $1\% \text{ y}^{-1}$   $\text{CO}_2$  increase  
18 experiment) are two metrics commonly used in climate model analysis and climate change  
19 study. The spread in their AOGCM estimates remains large from one phase of the CMIP  
20 project to another [Meehl and Coauthors, 2007]. The identification of the key mecha-  
21 nisms responsible for this spread and the quantification of their contributions constitute  
22 a necessary step in the improvement of climate change understanding and modeling.

23 For a given externally imposed radiative perturbation, the first-order transient surface  
24 temperature response is driven by two main properties of the climate system: the strength  
25 of the radiative response and the ocean thermal inertia [Dickinson, 1981; Hansen et al.,  
26 1984; Wigley and Schlesinger, 1985; Knutti and Hegerl, 2008]. Previous studies, based on  
27 individual model or multimodel analysis, attempted to estimate the role of these properties  
28 in the spread of AOGCMs responses. Multimodel studies have shown that the strength  
29 of the radiative feedback due to the cloud component constitutes the primary source  
30 of differences in the equilibrium temperature response [Soden and Held, 2006; Dufresne  
31 and Bony, 2008]. By decomposing the transient temperature response into the sum of  
32 contributions due to the Planck response, the forcing magnitude, the radiative feedbacks  
33 and the ocean heat uptake, Dufresne and Bony [2008] concluded that the main contributor  
34 to the spread in the TCR is the cloud feedback. Such conclusion is supported by individual

35 model studies suggesting that the atmosphere component is the major source of differences  
36 of transient responses (e.g. Williams et al. [2001]; Meehl et al. [2004]; Collins et al. [2007]).

37 However, by analyzing the inter-model correlation between the transient surface tem-  
38 perature response, the ECS and the mixing layer depth at high latitudes, Boé et al. [2009]  
39 suggested that the role of the deep-ocean heat uptake has been underestimated. The  
40 source of the spread of the transient responses is thus a topic of debate. Moreover, these  
41 studies are limited in two ways. First, they do not provide a quantitative estimate of  
42 the magnitude of the different contributions to the spread. Secondly, some key processes  
43 that can contribute significantly to the spread are not taken into account, mainly the  
44 tropospheric adjustment of the radiative forcing [Gregory and Webb, 2008; Colman and  
45 McAvaney, 2011] and the possible change in the global feedback strength during the tran-  
46 sition due to the impact of the deep-ocean heat uptake on the spatial structure of the  
47 surface temperature pattern [Winton et al., 2010; Geoffroy et al., 2012b, thereafter G12b].

48 To overcome these two main limitations, the use of a state-of-the-art energy-balance  
49 framework and a suitable statistical method are combined in order to investigate the  
50 different contributions of each climate system parameter/property to the spread in the  
51 responses of a given set of AOGCMs. After a presentation of the EBM framework (Section  
52 2), the statistical method is described (Section 3). This method is applied to 14 CMIP5  
53 AOGCMs and results are presented and discussed in Section 4.

## 2. Two-box EBM framework

54 The two-box energy-balance model with an efficacy factor of deep-ocean heat uptake  
55 (hereafter EBM- $\varepsilon$ ) predicts the time-evolution of the mean surface air temperature re-

56 sponse  $T$  and the deep-ocean temperature response  $T_0$  to an external radiative perturba-  
57 tion according to the following system of equations [Held et al., 2010, G12b]:

$$58 \quad C \frac{dT}{dt} = \mathcal{F} - \lambda T - \varepsilon \gamma (T - T_0), \quad (1)$$

$$59 \quad C_0 \frac{dT_0}{dt} = \gamma (T - T_0). \quad (2)$$

60

61 In this framework, the climate system is described by 3 radiative parameters, the forcing  
62 reference amplitude (such as  $\mathcal{F}_{2xCO_2}$ ), the equilibrium feedback parameter  $\lambda$  and the effi-  
63 cacy factor of deep-ocean heat uptake  $\varepsilon$ , and 3 thermal-inertia parameters, the first-layer  
64 (atmosphere/land/upper-ocean) surfacic heat capacity  $C$ , the second-layer (deep-ocean)  
65 surfacic heat capacity  $C_0$  and the heat exchange coefficient between the two layers  $\gamma$ .

66 Geoffroy et al. [2012a] (thereafter G12a) and G12b propose a calibration method to  
67 derive these 6 thermal parameters from an AOGCM step-forcing experiment. They show  
68 that this simple model represents fairly the transient response of a given AOGCM to a  
69 gradual increase of  $CO_2$ . The use of the EBM- $\varepsilon$  framework has several advantages. First,  
70 all parameters are adjusted consistently within a single framework. Then, the inclusion  
71 of the efficacy factor of deep-ocean heat uptake  $\varepsilon$  allows a refined representation of the  
72 radiative imbalance evolution likely resulting in a better estimation of the parameters  
73 driving the transient climate change. Thus one can assume that the set of thermal pa-  
74 rameters derived by this method can be used to quantify the contribution to the spread  
75 of the transient temperature responses simulated by a set of AOGCMs.

76 In the following of this section, a "process-oriented" decomposition of the transient  
77 surface temperature response is proposed. This decomposition allows to quantify the con-  
78 tributions of each process to the magnitude of the response and provides an insight of

79 the different mechanisms responsible for the spread of  $T(t)$ . As shown in G12b, the  
 80 surface temperature response can be decomposed as the sum of three contributions:  
 81  $T(t) = T_{eq}(t) + T_D(t) + T_U(t)$ . The first term is the instantaneous equilibrium tem-  
 82 perature  $T_{eq}(t) = \mathcal{F}(t)/\lambda$ . The remaining contribution  $T_U + T_D$  is the temperature per-  
 83 turbation associated with the climate system heat uptake  $T_H$  [Winton et al., 2010, G12a,  
 84 b] where  $T_U$  and  $T_D$  are the temperature perturbations associated respectively with the  
 85 upper- and the deep-ocean heat uptake [G12b]. More precisely,  $T_D$  can be decomposed  
 86 as the sum of two contributions,  $T_D^\lambda(t) = T_D(t)/\varepsilon$  representing the flux to deep ocean  
 87 and  $T_D^d(t) = T_D(t)(1 - 1/\varepsilon)$  representing the impact of the deep-ocean heat uptake on  
 88 the radiative imbalance due to the modification of the temperature pattern. The four  
 89 terms involved in this decomposition allows to distinguish the thermal fluxes at play in  
 90 the energy balance when associated with the scale factor  $\lambda$ . The sum  $T_H^\lambda = T_U + T_D^\lambda$   
 91 represents the instantaneous rate of heat storage of the climate system,  $-\lambda T_H^\lambda$  being the  
 92 top-of-the-atmosphere radiation imbalance. The contribution  $T_D^d$  is a deviation from  $T_{eq}$   
 93 due to the effect of the deep-ocean heat uptake on the strength of the radiative feedbacks  
 94 during the transition. The sum  $T_{eq} + T_D^d$  can be viewed as an apparent instantaneous  
 95 equilibrium surface temperature during the transition.

96 For the 14 CMIP5 AOGCMs listed in Table S1 in the auxiliary material, the multi-  
 97 model mean of the calibrated analytical surface temperature response in the 1%  $y^{-1}$  CO<sub>2</sub>  
 98 increase experiment and its decomposition in  $T_{eq}$ ,  $T_U$ ,  $T_D^\lambda$ , and  $T_D^d$  are plotted in Fig.  
 99 1. For comparison, the multimodel mean of the AOGCMs temperature responses is also  
 100 represented. The difference with the analytical solution is small (which is also the case for

101 individual model) supporting that the EBM framework is suitable for the present study.  
102 Note that this bias decreases during the second half of the simulations (period 70-140  
103 yr from 2xCO<sub>2</sub> to 4xCO<sub>2</sub>). The TCR and the ECS are respectively of the order of 2 K  
104 and 3.5 K. The inter-model standard deviation of the ECS (about 1 K) is larger than  
105 the standard deviation of the TCR (about 0.4 K) because the ocean heat uptake reduces  
106 the spread [Raper et al., 2002]. This results from the dependency between  $T_{eq}$  and the  
107 negative contribution  $T_H$ . In particular, both are scaled by a factor  $1/\lambda$ . The term  $T_H$   
108 is dominated by the deep-ocean heat uptake temperature representing the flux to deep  
109 ocean  $T_D^\lambda$ , with an ensemble mean amplitude of  $-1$  K. The mean amplitude of  $T_D^d$  is as  
110 large as the mean amplitude of  $T_U$  with a value of about  $-0.3$  K but is associated with  
111 a larger spread, suggesting a non negligible role of the efficacy factor of deep-ocean heat  
112 uptake to the spread.

113 The decomposition of the transient surface temperature response presented here is dif-  
114 ferent from the one of Dufresne and Bony [2008]. Their decomposition is expressed with  
115 respect to the Planck feedback parameter  $\lambda_P$  rather than  $\lambda$ . Considering that  $\lambda_P$  is  
116 roughly model independent, the spread of each term is then associated with one parame-  
117 ter only (within the framework of a one-box EBM) but depends also on  $T$ . Because these  
118 terms are not a priori independent, their respective variance cannot be simply added, and  
119 the resulting decomposition may be misleading. A more accurate quantification of the  
120 contribution of each physical parameter to the spread of the temperature responses may  
121 be derived based on the statistical method described in the next section.

### 3. Statistical method

122 The contribution of each thermal property to the spread of the multimodel global surface  
123 warming in the 1%  $y^{-1}$  CO<sub>2</sub> experiment is investigated via a multifactor analysis of  
124 variance (e.g. Christensen, 1996, p.331). The parameters driving a transient climate  
125 change are assumed to be the 6 parameters of the EBM- $\varepsilon$ . The transient temperature  
126 response  $T$  is a time-dependant function of these 6 parameters:

$$127 \quad T = f(\mathcal{F}_{2xCO_2}, \lambda, \gamma, C, C_0, \varepsilon). \quad (3)$$

128 The function  $f$  is assumed to be the analytical solution of the EBM- $\varepsilon$  described in G12b.  
129 For each of the 14 AOGCMs used in this study, the calibrated values of the 6 parameters  
130 are summarized in Table S1.

131 In order to estimate the contribution of each parameter to the spread of  $T$ , we need  
132 to allow each parameter to vary individually. For this purpose, an ensemble of  $N_0 =$   
133  $14^6$  values of the temperature response  $\{T_{i,j,k,l,m,n}\}$  is computed at each time step by  
134 considering all possible combinations of the AOGCM parameters:

$$135 \quad T_{i,j,k,l,m,n} = f(\mathcal{F}_{2xCO_2,i}, \lambda_j, \gamma_k, C_l, C_{0,m}, \varepsilon_n). \quad (4)$$

136 where the subscript  $i$  denotes that the forcing parameter value is the one of the  $i^{th}$   
137 AOGCM and similarly for  $j, k, l, m, n$ . The use of the all-parameter combinations en-  
138 semble  $\{T_{i,j,k,l,m,n}\}$  assumes that the parameters are independent which is roughly the  
139 case except potentially for  $C$  and  $\gamma$  [G12b], but  $C$  does not play an important role, as it  
140 will be shown in the following. Also, a dependency between  $\varepsilon$  and  $T_{eq}$  (i.e.  $\mathcal{F}/\lambda$ ) may exist.  
141 Following the analysis of variance method,  $T$  is decomposed in the sum of one-variable



142 functions:

$$\begin{aligned}
 143 \quad T &= f_0 + f_1(\mathcal{F}_{2\times\text{CO}_2}) + f_2(\lambda) + f_3(\varepsilon) + f_4(C) \\
 144 \quad &+ f_5(C_0) + f_6(\gamma) + I(\mathcal{F}_{2\times\text{CO}_2}, \lambda, \varepsilon, C, C_0, \gamma), \tag{5}
 \end{aligned}$$

146 where  $I$  is an interaction term (including first-order interactions, second-order, etc). This  
 147 decomposition is exact but  $I$  is potentially significant. The best approximation of  $T$  over  
 148 the set of values considered is then obtained by computing, from the  $\{T_{i,j,k,l,m,n}\}$ , the  
 149 mean value  $\widehat{f}_0 = \overline{T}$ , the function  $\widehat{f}_1$  such that:

$$150 \quad \widehat{f}_1(\mathcal{F}_{2\times\text{CO}_2,i}) = \frac{1}{N_2 \dots N_6} \sum_{j,k,l,m,n} (T_{i,j,k,l,m,n} - \overline{T}), \tag{6}$$

151 and similarly, the functions  $\widehat{f}_2$  to  $\widehat{f}_6$ , where  $N_1, \dots, N_6$  denotes respectively the number  
 152 of values taken by the parameters  $\mathcal{F}, \dots, \varepsilon$  (in our case,  $N_1 = \dots = N_6 = 14$ ). The  
 153 interaction term  $I$  can then be estimated as a residual from Eq. (5).

154 The variance  $Var(T)$  of the ensemble  $\{T_{i,j,k,l,m,n}\}$  can be decomposed as the following:

$$\begin{aligned}
 155 \quad Var(T) &= \frac{1}{N} \sum_{i,j,k,l,m,n} (T_{i,j,k,l,m,n} - \overline{T})^2, \\
 156 \quad Var(T) &= \frac{1}{N_1} \sum_i \widehat{f}_1(\mathcal{F}_{2\times\text{CO}_2,i})^2 + \dots \\
 157 \quad &+ \frac{1}{N_6} \sum_n \widehat{f}_6(\varepsilon_n)^2 + Var(I), \tag{7}
 \end{aligned}$$

$$158 \quad Var(T) = (\widehat{c}_{\mathcal{F}} + \dots + \widehat{c}_{\varepsilon} + \widehat{c}_I) Var(T), \tag{8}$$

160 where  $\widehat{c}_x$  denotes the estimated contribution of the parameter  $x$  to the variance of  
 161  $\{T_{i,j,k,l,m,n}\}$ :

$$162 \quad \widehat{c}_x = \frac{1}{Var(T)} \frac{1}{N_x} \sum_i \left[ \frac{1}{N_y \dots N_z} \sum_{j \dots n} (T_{i,j,k,l,m,n} - \overline{T}) \right]^2 \tag{9}$$

163 Note that the term  $\widehat{c}_I$  is somewhat more complicated and not explicitly written here (see  
 164 e.g. Christensen, 1996). In the case of two models, the present method is equivalent to

165 the factorial method [Montgomery, 2005] used by Teller and Levin [2008] to evaluate the  
166 relative contributions of thermodynamic conditions and microphysical characteristics to  
167 variations in precipitation.

#### 4. Contributions of the physical parameters.

168 The frequency distributions of the TCR and the ECS obtained for all-parameter com-  
169 binations ensemble ( $14^6$  elements for the TCR and  $14^2$  elements for the ECS) are shown  
170 in Fig. 2. Both distributions are highly skewed with a long tail due to the non linear  
171 relationship between the climate sensitivity and the feedback factor [Knutti and Hegerl,  
172 2008]. The time-evolution of the variance of the inter-model and of the all-parameter com-  
173 binations ensemble for  $T(t)$  and  $T_{eq}(t)$  is represented in Fig. 3a. The variance of  $T_{eq}(t)$   
174 increases as a square function of time and roughly similarly for  $T(t)$ . In each case, the  
175 spread of the all-parameter combinations ensemble is larger than the inter-model spread  
176 (see also Fig. 2). Nevertheless, the all-parameter combinations variances  $Var(T)$  and  
177  $Var(T_{eq})$  (e.g. respectively  $1.15 \text{ K}^2$  and  $5.87 \text{ K}^2$  at  $4x\text{CO}_2$ ) are well within the 5-95%  
178 confidence interval of their respective inter-model spread (respectively  $0.42$  to  $1.6 \text{ K}^2$  and  
179  $2.54$  to  $9.60 \text{ K}^2$  at  $4x\text{CO}_2$ ). Figure 3b,c show the time-evolution of the contributions  
180 associated with the thermal parameters and the interaction term to the spread of  $T(t)$ .  
181 Note that the contributions to  $T_{eq}(t)$  do not vary in time. The magnitude of the different  
182 contributions to the TCR and the ECS are summarized in Fig. 3d. The interaction term  
183 explains about 3 % and 1 % of the spread respectively of the TCR and of the ECS. These  
184 low values suggest that the analysis of variance decomposition is accurate to quantify the  
185 contributions to the spread in the responses.

186 The equilibrium temperature response is a function of the adjusted radiative forcing  
187 and the equilibrium radiative feedback parameter only. Their respective contributions to  
188 the spread of the ECS are respectively of 12 % and 87 %. The inter-model spread of the  
189 radiative feedback parameter is by far the main contributor to the spread of the ECS.  
190 Many studies suggest that the spread of  $\lambda$  is due to the cloud feedback [Soden and Held,  
191 2006; Dufresne and Bony, 2008]. The methodology presented here could be extended  
192 to quantify the contribution of each independent radiative feedback (water vapor plus  
193 lapse rate, cloud and surface albedo) by using a decomposition of the global radiative  
194 feedback parameter. Similarly, a decomposition of the adjusted radiative forcing could be  
195 performed in order to evaluate the contribution of fast adjustments to the spread.

196 During the transition, the total contribution of  $\mathcal{F}_{2xCO_2}$  and  $\lambda$  is reduced due to the  
197 role of the other parameters. After few decades,  $\lambda$  remains the main contributor to the  
198 spread, but less strongly than in equilibrium, with a value of 54 % at the time of  $2xCO_2$ .  
199 On the contrary, the transient contribution of  $\mathcal{F}_{2xCO_2}$  is enhanced in comparison with the  
200 equilibrium one. It decreases with time and reach a value of the order of 28 % after 70  
201 years of simulations. This emphasizes the importance of the forcing magnitude during a  
202 climate transition and the uncertainty associated with the tropospheric adjustment. The  
203 efficacy  $\varepsilon$  is the third factor that contributes most to the TCR spread with a  $2xCO_2$  value  
204 of 10 %. This support Winton et al. [2010]’s finding that  $\varepsilon$  needs to be taken into account  
205 in EBM studies. Finally, the spread of the TCR is mostly due to the radiative parameters  
206  $\lambda$ ,  $\mathcal{F}_{2xCO_2}$  and  $\varepsilon$  with a total value of about 92 %. Note that they are also the main

207 contributors to the spread of  $T_U$ ,  $T_D^\lambda$  and  $T_U^d$  (not shown). The efficacy  $\varepsilon$  is the main  
208 contributor for  $T_D^d$  whereas the spread of  $T_U$  and  $T_D^\lambda$  is mainly dominated by  $\lambda$ .

209 The contribution of  $\gamma$  is small, with a value of 4 % at 70 yr. The time-evolution of  
210 its contribution is similar to the one of  $\varepsilon$ , both being associated with a common process,  
211 the deep-ocean heat uptake. The contribution of  $C_0$  increases in time and decreases back  
212 after few centuries (not shown). This contribution is very small with a value of about 1  
213 % at 70 yr. As expected, the contribution of  $C$  is negligible after few years. Indeed,  $T_U$   
214 contributes little to the magnitude of  $T$  and is characterized by a very small inter-model  
215 spread. During the first years, for which the variance is negligible, the spread is mainly  
216 explained by  $C$  and  $\mathcal{F}_{2\times\text{CO}_2}$ . This may be due to the fact that initially, the temperature  
217 tendency is equal to  $\mathcal{F}/C$ . Note that the contribution associated with  $\varepsilon$ ,  $C_0$  and  $C$ , even  
218 if small for long (unrealistic) time-integration, doesn't tend towards 0 whereas the one  
219 associated with  $\gamma$  does. Indeed, the asymptotic temperature response deviation associated  
220 with the ocean heat uptake  $T - T_{eq}$  is equal to  $(C + \varepsilon C_0)/\lambda$  and is independent of  $\gamma$ .

## 5. Conclusion

221 In this paper, it is shown that the combination of an energy-balance framework and  
222 the analysis of variance method allows to quantify the sources of the spread in climate  
223 change experiments. Disregarding that radiative processes are not independent of ocean  
224 processes, our results strongly support that atmospheric processes constitute the major  
225 source of uncertainty in climate model projections. These uncertainties manifest them-  
226 selves in several ways, primarily in the strength of the radiative feedbacks to the surface  
227 warming but also in the tropospheric adjustment and to a lesser extent in the strength

228 of the local radiative feedbacks in the region where the warming is slowed by deep-ocean  
229 heat uptake relatively to other regions.

230 The results presented here are consistent with the conclusion of Dufresne and Bony  
231 [2008]. They concur that the spread in the transient temperature response is mainly  
232 due to the radiative feedbacks and thus clouds, secondly to the forcing and then to the  
233 ocean heat uptake. Note that the method used in both studies are similar in the sense  
234 that they are based on an energy-balance framework. However, contrary to Dufresne  
235 and Bony [2008], the present study supports an increased importance of the role of the  
236 adjusted radiative forcing as a contributor and a very low contribution of the ocean heat  
237 uptake. The latter may be explained by the addition of the efficacy factor that damps  
238 the previous estimates of the contributions associated with the heat exchange coefficient.  
239 Finally, this study is consistent with the statement that the cloud field constitutes the most  
240 critical component in climate modeling by introducing uncertainties at various spatial and  
241 temporal scales.

242 **Acknowledgments.** We gratefully thank Gilles Bellon, Herve Douville, Julien Boe,  
243 Laurent Terray for discussions that helped us to improve the manuscript. This work was  
244 supported by the European Union FP7 Integrated Project COMBINE.

## References

245 Boé, J., A. Hall, and X. Qu, 2009: Deep ocean heat uptake as a major source of spread  
246 in transient climate change simulations. *Geophys. Res. Lett.*, **36**, L22701.

247 Christensen, R., 1996: Analysis of variance, design, and regression: applied statistical  
248 methods. *Chapman & Hall*, 587pp.

249 Collins, M., C. M. Brierley, M. MacVean, B. B. B. Booth, and G. R. Harris, 2007: The  
250 sensitivity of the rate of transient climate change to ocean physics perturbations. *J. of*  
251 *Climate*, **20**, 2315–2320.

252 Colman, R. A. and B. J. McAvaney, 2011: On tropospheric adjustment to forcing and  
253 climate feedbacks. *Clim. Dyn.*, **36**, 1649–1658.

254 Dickinson, R., 1981: Convergence rate and stability of ocean-atmosphere coupling schemes  
255 with a zero-dimensional climate model. *J. Atmos. Sci.*, **38**, 2112–2120.

256 Dufresne, J.-L. and S. Bony, 2008: An assessment of the primary sources of spread of  
257 global warming estimates from coupled atmosphere-ocean models. *J. Atmos. Sci.*, **21**,  
258 5135–5144.

259 Geoffroy, O., D. Saint-Martin, D. J. L. Olivié, A. Voldoire, G. Bellon, and S. Tyteca,  
260 2012a: Transient climate response in a two-box energy-balance model. Part I: analytical  
261 solution and parameter calibration using CMIP5 AOGCM experiments. *submitted to J.*  
262 *of Climate*.

263 Geoffroy, O., D. Saint-Martin, G. Bellon, A. Voldoire, D. J. L. Olivié, and S. Tyteca,  
264 2012b: Transient climate response in a two-box energy-balance model. Part II: repre-  
265 sentation of the efficacy of deep-ocean heat uptake and validation for CMIP5 AOGCMs.  
266 *submitted to J. of Climate*.

267 Gregory, J. and M. Webb, 2008: Tropospheric adjustment induces a cloud component in  
268 CO<sub>2</sub> forcing. *J. of Climate*, **21**, 58–71.

269 Hansen, J., A. Lacis, D. Rind, G. Russell, P. Stone, I. Fung, R. Ruedy, and J. Lemer.,  
270 1984: Climate sensitivity: Analysis of feedback mechanisms. *Climate Processes and*  
271 *Climate Sensitivity eds., Washington, D.C.: American Geophysical Union*, pp 130–163.

272 Held, I. M., M. Winton, K. Takahashi, T. Delworth, F. Zeng, and G. K. Vallis, 2010:  
273 Probing the fast and slow components of global warming by returning abruptly to  
274 preindustrial forcing. *J. of Climate*, **23**, 2418–2427.

275 Knutti, R. and G. C. Hegerl, 2008: The equilibrium sensitivity of the Earth’s temperature  
276 to radiation changes. *Nature Geoscience*, **1**, 735–743.

277 Meehl, G. A. and Coauthors, 2007: Global climate projection. climate change 2007: The  
278 scientific basis. *Cambridge University Press*, 747–846.

279 Meehl, G. A., W. M. Washington, J. M. Arblaster, and A. Hu, 2004: Factors affecting  
280 climate sensitivity in global coupled models. *J. of Climate*, **17**, 1584–1596.

281 Montgomery, D. C. 2005: Design and Analysis of Experiments, 6th ed., *John Wiley &*  
282 *Sons*, New York, 684 pp.

283 Raper, S. C. B., J. M. Gregory, and R. J. Stouffer, 2002: The role of climate sensitivity  
284 and ocean heat uptake on aogcm transient temperature response. *J. of Climate*, **15**,  
285 124–130.

286 Soden, B. J. and I. M. Held, 2006: An assessment of climate feedbacks in coupled ocean-  
287 atmosphere models. *J. of Climate*, **19**, 3354–3360.

288 Teller, A. and Levin, Z., 2008: Factorial method as a tool for estimating the relative contri-  
289 bution to precipitation of cloud microphysical processes and environmental conditions.  
290 *J. of Climate*, **113**, 3354–3360.

- 291 Wigley, T. M. L. and M. E. Schlesinger, 1985: Analytical solution for the effect of increas-  
292 ing CO<sub>2</sub> on global mean temperature. *Nature*, **315**, 649–652.
- 293 Williams, K. D., C. A. Senior, and J. F. B. Mitchell, 2001: Transient climate change in  
294 the Hadley centre models: the role of physical processes. *J. of Climate*, **14**, 2659–2674.
- 295 Winton, M., K. Takahashi, and I. M. Held, 2010: Importance of ocean heat uptake efficacy  
296 to transient climate change. *J. of Climate*, **23**, 2333–2344.



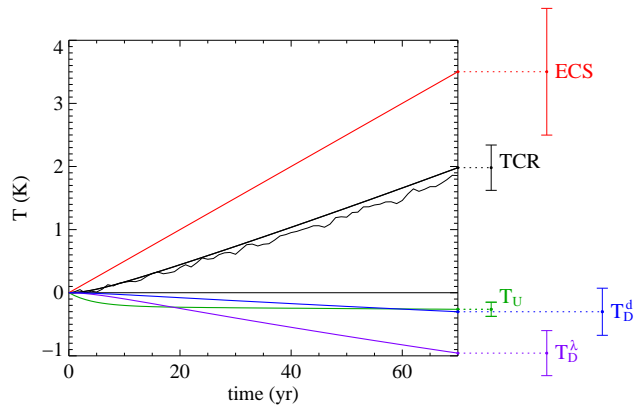


**Figure 1.** Time-evolution of the multimodel mean of the surface temperature response (thin black) of the  $1\% \text{ y}^{-1} \text{ CO}_2$  increase experiment until the time of  $2\text{xCO}_2$  (70 yr), of the calibrated analytical surface temperature response (thick black) and its decomposition in  $T_{eq}(t)$  (red),  $T_U$  (green),  $T_D^\lambda$  (purple) and  $T_D^d$  (blue). The vertical bars at right indicate the  $\pm 1$  inter-model standard deviation for each variable at the time of  $2\text{xCO}_2$ .

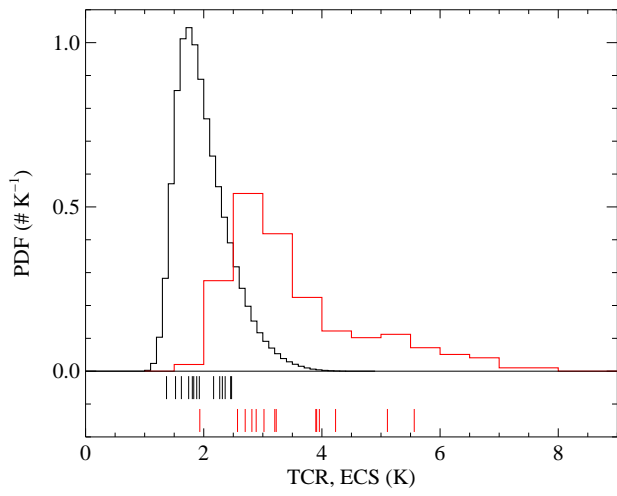


**Figure 2.** Probability density functions of the TCR (black) and the ECS (red) obtained for all combinations of the parameters of the set of AOGCMs. The vertical lines at bottom indicate the individual model analytical values of the TCR (black) and the ECS (red).

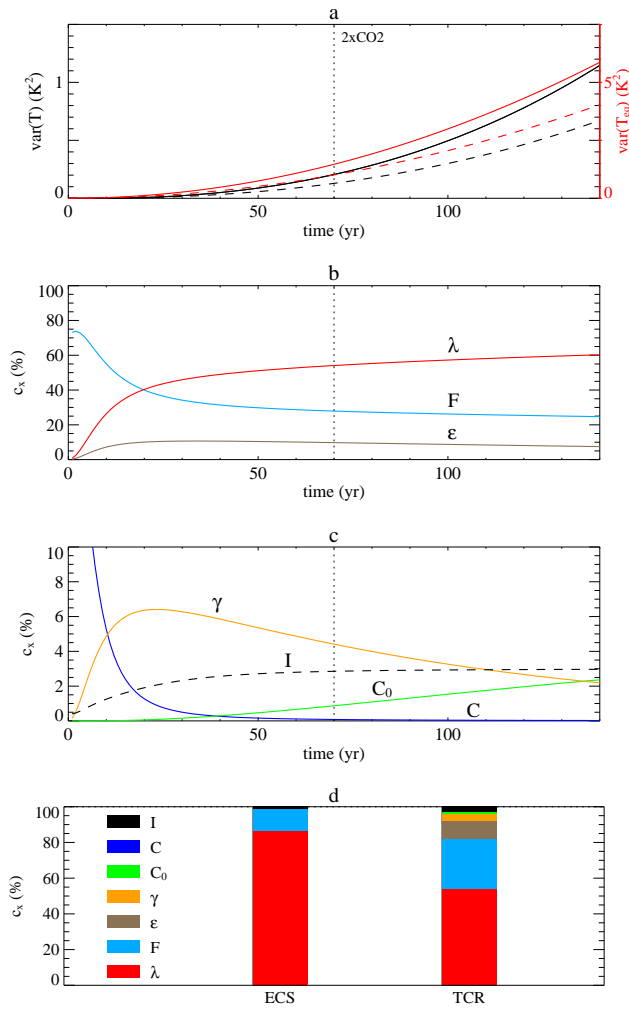


**Figure 3.** (a) Time-evolution of the variances of the multimodel analytical surface temperature response (black, dashed), and of the all-parameter combinations surface temperature response (black, solid) and equilibrium temperature response (red). Time-evolution (over 140 yr) of the contribution (%) to the spread of the transient surface temperature responses associated with (b) the radiative parameters  $\mathcal{F}_{2\times\text{CO}_2}$ ,  $\lambda$ , and  $\varepsilon$  and (c) the thermal inertia parameter  $C$ ,  $C_0$  and  $\gamma$ . The contribution of the interaction term is also plotted (dashed black line) on (c). (d) Contribution of each parameters and of the interaction term to the ECS and the TCR.